Antagonistic model of random sequential adsorption of two-species discorectangles

Nikolai Lebovka [1,*] Leonid A. Bulavin [2] and Nikolai Vygornitskii [1]

[1] *Laboratory of Physical Chemistry of Disperse Minerals, F. D. Ovcharenko Institute of Biocolloidal Chemistry, NAS of Ukraine, Kyiv 03142, Ukraine*

[2] *Faculty of Physics, Taras Shevchenko National University of Kyiv, 4, Akademika Glushkova Ave., Kyiv 03022, Ukraine*

(Received 16 February 2026; accepted 13 July 2026; published 3 August 2026)

An antagonistic random sequential adsorption (RSA) model is investigated to describe competitive adsorption on an adsorbent surface by particles of two types, a and b. The degree of competition is characterized by the probability $p_a (p_b = 1 - p_a)$ that an arriving particle is of type a. Particles of both types are modeled as discorectangles with aspect ratio $\varepsilon = l/d$, where l and d denote the particle length and thickness, respectively. Each particle is surrounded by a shell of thickness δ, which induces repulsive interactions between particles of opposite types. This repulsion leads to the spontaneous formation of clusters consisting of particles of a single type, separated from clusters of the opposite type by cavities of thickness approximately 2δ. The mechanisms governing the formation of the adsorption layer and the resulting jamming coverage are analyzed. In addition, the dependence of the shell percolation threshold, δ_c, on the probability p_a is examined for different values of the shell thickness δ and the aspect ratio ε.

DOI: 10.1103/9gy6-2d3b

I. INTRODUCTION

In recent years, various types of self-assembled structures formed by packings of elongated particles on two-dimensional (2D) substrates have attracted considerable attention. Such structures have promising applications in memory devices, surfaces with controlled wettability, transparent electrodes for optoelectronics, and sensor materials. Self-assembly can occur through the process of random sequential adsorption (RSA), which involves the irreversible deposition of immobile particles on a 2D substrate [1,2]. In the RSA model, particles are deposited sequentially, overlap is prohibited, and adsorption terminates when the maximum surface coverage φ_J is reached.

The RSA model is a highly effective tool for describing the deposition of nanoparticles, bioparticles, macromolecules, and colloidal particles [3,4]. RSA of elongated particles is a complex problem that continues to attract significant research interest [5]. Previous studies have examined RSA packings of rectangles [6,7], discorectangles [8,9], ellipses [10–13], and other elongated objects [14–16] with different aspect ratios (length-to-width ratio $\varepsilon = l/d$). In many cases, interesting nonmonotonic dependencies of $\varphi_J(\varepsilon)$ have been observed. For example, in the case of unoriented discorectangles, the maximum value of $\varphi_J \approx 0.584$ occurs at $\varepsilon \approx 1.84$, after which φ_J decreases monotonically with further increases in ε [8]. This behavior has been attributed to the competition between orientational degrees of freedom and excluded area effects [17]. For multicomponent mixtures of particles with different sizes and shapes, several variants of competitive and multistep RSA models have been investigated. In competitive models, particles of different types are selected with a fixed probability, whereas in multistep models, substrates are sequentially coated with different particle types. Previous works have studied competitive RSA deposition for disks of different sizes [18–21], as well as mixtures of disks and discorectangles [22]. Multistep RSA deposition on heterogeneous, partially precoated surfaces has also been extensively discussed [3,23–26]. In particular, it has been demonstrated that preadsorption of small disks significantly affects the adsorption of large disks and reduces their adsorption rate [27,28]. In two-step adsorption models of mixtures of disks and discorectangles, discorectangles are adsorbed first and disks second (SD model), or vice versa (DS model). In both cases, the presence of preadsorbed particles constrains the maximum allowable disk diameter $D_{\max}$ (SD model) or the maximum aspect ratio $\varepsilon_{\max}$ (DS model) [26].

To date, a wide range of multicomponent RSA models has been extensively studied. A one-dimensional (1D) lattice model involving competition between several irreversible reactions was analyzed in [29], where cooperative effects were taken into account by allowing reaction rates to depend on the states of neighboring sites. A modified 1D RSA model describing the deposition of two distinct particle types, a and b, onto a lattice was proposed in [30], incorporating the constraint that particles of different types cannot occupy adjacent sites. More complex multisite two-dimensional (2D) models on a square lattice have also been investigated. In such models, empty lattice sites are filled randomly, provided that specific nearest-neighbor conditions are satisfied [31]. The

*Contact author: lebovka@gmail.com

Published by the American Physical Society under the terms of the Creative Commons Attribution 4.0 International license. Further distribution of this work must maintain attribution to the author(s) and the published article's title, journal citation, and DOI.

jamming and percolation behavior in RSA of binary mixtures of monomers and square-shaped particles square lattice with varying linear size ratio R and relative flux F have also been studied [32]. In the context of competitive adsorption, the formation of conducting monolayers with tunable conductance has been demonstrated. A competitive 2D RSA model on a square lattice involving two antagonistic particle types, a and b, was analyzed in [33]. The degree of competition between particle types is governed by the probability p_a that the next arriving particle is of type a. Antagonistic interactions are introduced by allowing particles of one type to adsorb freely, whereas particles of the opposite type can adsorb only beyond a certain distance defined by the thickness of a repulsive shell δ [33]. However, to the best of our knowledge, a continuous version of the competitive antagonistic model for discorectangle particles has likely not yet been considered in the literature. In our work, the competitive RSA model with two antagonistic particle types, a and b, both shaped as discorectangles is investigated. The degree of competitive adsorption between the two particle types is governed by the probability p_a that the next particle arriving at the surface will be of type a. Antagonism between particle types is introduced by allowing particles of one type to adsorb freely on the surface, while particles of the opposite type may adsorb only at a certain distance determined by the thickness of the repulsive shell δ.

The remainder of this paper is organized as follows. Section II introduces the model and describes the methodology for calculating the jamming coverage and the critical shell thickness associated with percolation cluster formation. Section III presents the dependencies of jamming coverage and percolation shell thickness on the model parameters. Section IV provides the conclusions.

II. MODEL AND DETAILS OF CALCULATION

A. Model formulation

The model of simultaneous adsorption of two types of particles, a and b, on the surface of an adsorbent. The values of r_a and r_b denote the rates at which particles a and b reach the surface. In this model the values $p_a = r_a/(r_a + r_b)$ and $p_b = r_b/(r_a + r_b) = 1 - p_a$ are the probabilities that the next particle arriving at the surface will be of type a or b, respectively [33]. Particles a and b are modeled as discorectangles with length l and thickness d, characterized by the aspect ratio $\varepsilon = l/d$. In the special case $\varepsilon = 1$, the discorectangle reduces to a disk. The adsorbent surface is represented by a square region of size L with periodic boundary conditions. Simulations were performed for $\varepsilon = 1 - 10$, and all lengths in the model are expressed in units of d.

Adsorption of each particle type was carried out according to the rules of the random sequential adsorption (RSA) model [1]. Additionally, the following repulsion rule between particles of opposite types is introduced. Each particle is surrounded by a shell of thickness δ, which prevents adsorption of opposite-type particles within a distance where their shells would overlap.

Figure 1 shows typical packings of discorectangles for the same shell thickness δ but different aspect ratios ε. During adsorption, clusters of particles of the same type self-assemble, separated from clusters of the opposite type by cavities of thickness 2δ (unshaded areas in the figure). Since the shells of particles of opposite types are nonoverlapping, the minimum separation between a and b domains is at least 2δ, a condition that is strictly valid only near contact or in the jamming regime.

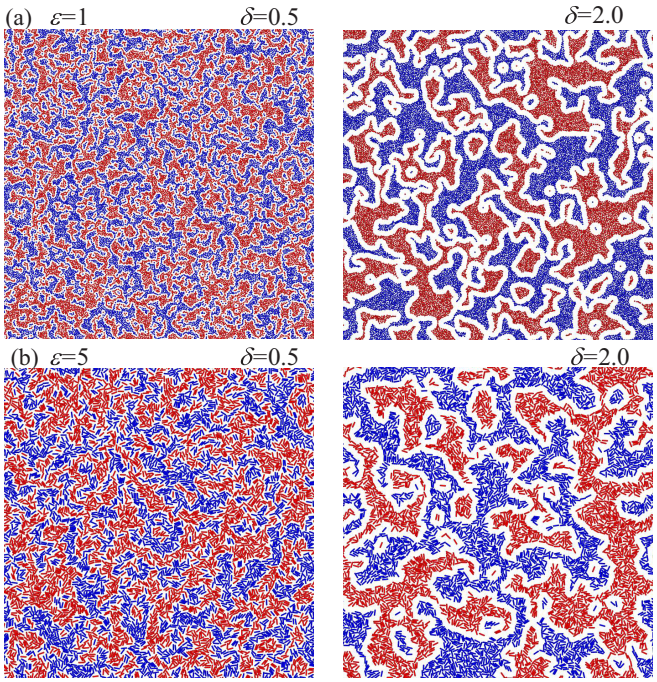


FIG. 1. Examples of packings of discorectangles with the same shell thickness $\delta = 0.5, 2.0$ and different aspect ratios $\varepsilon = 1$(a), and $\varepsilon = 5$(b). Particles of type a are shown in red and type b in blue. The probability $p_a = 0.5$, and the size of the square region is $L = 256$.

B. Evaluation of jamming coverage

The surface coverage by particles a or b was calculated as

$$\varphi^{a(b)} = N^{a(b)}A/L^2,$$

where $N^{a(b)}$ is the number of adsorbed particles of type a (b), and $A = (\varepsilon - 1 + \pi/4)d^2$ is the area of a discorectangle.

During simulations, the time dependences $\varphi^a(t)$, $\varphi^b(t)$, and the total coverage $\varphi(t) = \varphi^a(t) + \varphi^b(t)$ are calculated. To simplify numerical representation, time was normalized as

$$t = N/L^2,$$

where N is the total number of deposition attempts for both particle types.

The maximum value of t reached in this work was $t \approx 10^6$. Even at such large t, deposition of both particle types remains possible. Therefore, to estimate the jamming coverage $\varphi_J = \varphi(t \to \infty)$, we employed the standard approximation relation [34,35]:

$$\varphi(t) \sim \varphi_J - \frac{c}{t^\alpha}, \tag{1}$$

where the parameters c and α depend on the aspect ratio ε.

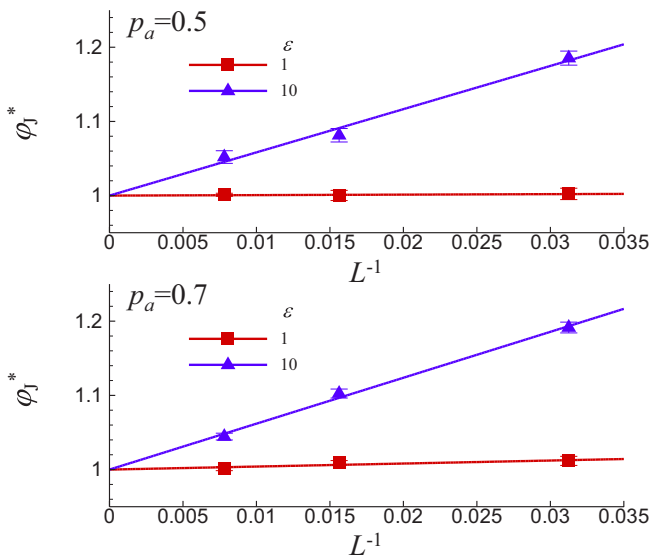


FIG. 2. Dependence of the normalized value $\varphi_J^* = \varphi_J(L)/\varphi_J(L \to \infty)$ on the inverse system size L^{-1} for aspect ratios $\varepsilon = 1$ and $\varepsilon = 10$ and two probability values $p_a = 0.5$ and 0.7. The shell thickness is $\delta = 0.5$. Symbols correspond to system sizes $L = 32, 64, 128$.

This approximation was applied both to the total coverage φ_J and to the partial coverages φ_J^a and φ_J^b.

To assess finite-size effects, the dependence of φ_J on L is examined. Figure 2 shows examples of normalized coverage $\varphi_J^* = \varphi_J(L)/\varphi_J(L \to \infty)$ versus inverse system size L^{-1} for aspect ratios $\varepsilon = 1$ and $\varepsilon = 10$ and probabilities $p_a = 0.5, 0.7$. For $\varepsilon = 1$ (disks), the relative error in φ_J is nearly independent of L and below 1%. For $\varepsilon = 10$, the error decreases with increasing L but remains more pronounced. Most calculations were performed at $L = 128$, for which the error in φ_J does not exceed 5%.

C. Calculation of percolation shell thickness δ_c

In the RSA model, the formation of a percolation cluster through direct contact between particles is unlikely. Therefore, percolation in the adsorption layer can occur only when connectivity between particles arises due to the overlap of specific shells around particles of a given type. To achieve percolation, it is necessary to introduce an effective connectivity criterion, often represented by an artificial percolation shell that allows for overlap. For example, in colloidal systems, this effect may arise from the overlap of electrical double layers surrounding the particles [36]. In this study, we assume that percolation shells of thickness δ_c form only around particles of type a, and thus the calculation of the percolation shell thickness was performed exclusively for this particle type. The method for determining the critical shell thickness δ_c is described in detail in our previous work [37]. The critical shell thickness was determined for configurations obtained at $L = 128$ and $t = 10^5$, which are close to the jamming point (see Fig. 2). It was defined as the minimum shell thickness at which a percolating cluster appears. Because the particle concentration remains below the true jamming concentration, the calculated critical shell thicknesses represent upper bounds on the true critical shell thickness.

D. Statistics

The numerical results presented in this paper are obtained by averaging over 10–50 independent packings of discorectangles. The whiskers on the graphs represent the standard errors of the mean. If not explicitly indicated, their size is comparable to that of the markers.

III. RESULTS AND DISCUSSION

A. Jamming

Figure 3 shows typical time dependencies of the coverage φ for disks ($\varepsilon = 1$) of types a and b, along with the corresponding derivatives $d\varphi/d\log(t)$, for two probability values, $p_a = 0.5$ and 0.7. For $p_a = 0.5$, the coverages of the individual components and their derivatives nearly coincide, indicating a fully balanced system with respect to the two particle types. Adsorption at $p_a = 0.5$ represents the case of maximum competition between particle types. Analysis of the derivatives $d\varphi/d\log(t)$ suggests that the adsorption process can be divided into two stages, with the boundary at the maximum ($t \approx 1$). The first stage ($t < 1$) is characterized by the formation of cluster growth centers for each particle type, while the second stage ($t > 1$) corresponds to the enlargement of these clusters.

For $p_a = 0.7$, adsorption is dominated by particles of type a, as clearly seen in the time dependences of $\varphi^a(t)$ and $\varphi^b(t)$. Analysis of the derivatives $d\varphi/d\log(t)$ indicates that at the initial stage ($t \lesssim 10^{-2}$), the rates of formation of cluster growth centers are nearly identical for both particle types. However, as t increases, the formation of new clusters of type b is largely suppressed by type a particles around $t \approx 10^{-1}$. Subsequently, the increase in φ^b occurs primarily through the growth of existing clusters of type b.

Figure 4 shows the jamming coverages φ_J^a and φ_J^b as functions of p_a for particles with aspect ratios $\varepsilon = 1$ (a) and 10 (b), and shell thicknesses $\delta = 0.1, 0.5, 1, 2$. For all values of δ, φ_J^a increases with increasing p_a, while φ_J^b decreases toward zero. In this model, the jamming coverage is completely symmetric with respect to $p_a = 0.5$, and the limiting values $p_a = 0$ and $p_a = 1$ correspond to the single-component RSA model, where the maximum jamming coverage is observed for all δ. At the limiting points, the equality $\varphi_J^a(p_a = 1) \equiv \varphi_J^b(p_a = 0)$ holds. The maximum jamming coverage at the limiting points depends on the aspect ratio ε. For example, $\varphi_J^a \approx 0.547$ for $\varepsilon = 1$ and $\varphi_J^a \approx 0.480$ for $\varepsilon = 10$.

The minimum total jamming coverage for both particle types occurs at $p_a = 0.5$ and decreases with increasing δ. This behavior arises because p_a acts as a parameter regulating the deviation of the two-component system from the single-component RSA model. At $p_a = 0.5$, the minimum coverage is observed, and it decreases as δ increases due to the enlargement of cavities between clusters of different particle types, which reduces φ_J^a and φ_J^b.

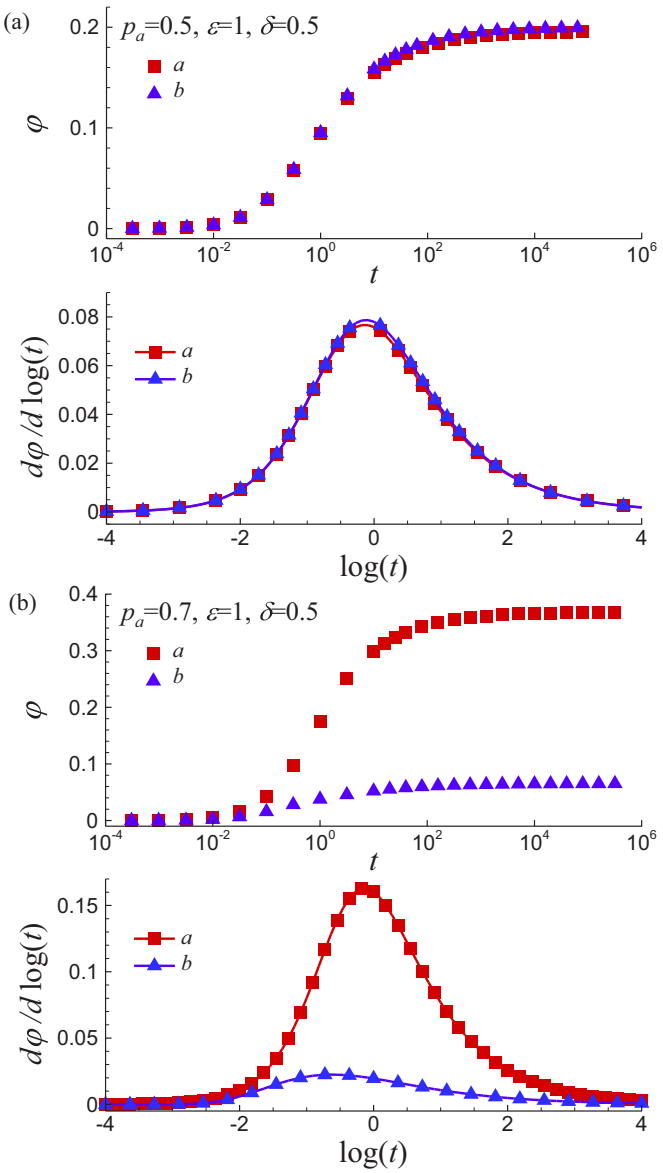


FIG. 3. Dependence of the coverage φ for particles of two types, a and b, on time t, and the corresponding derivatives $d\varphi/d\log(t)$ with respect to the decimal logarithm of time $\log(t)$, for two probability values $p_a = 0.5$ (a) and 0.7 (b). System size $L = 128$, aspect ratio $\varepsilon = 1$, and shell thickness $\delta = 0.5$.

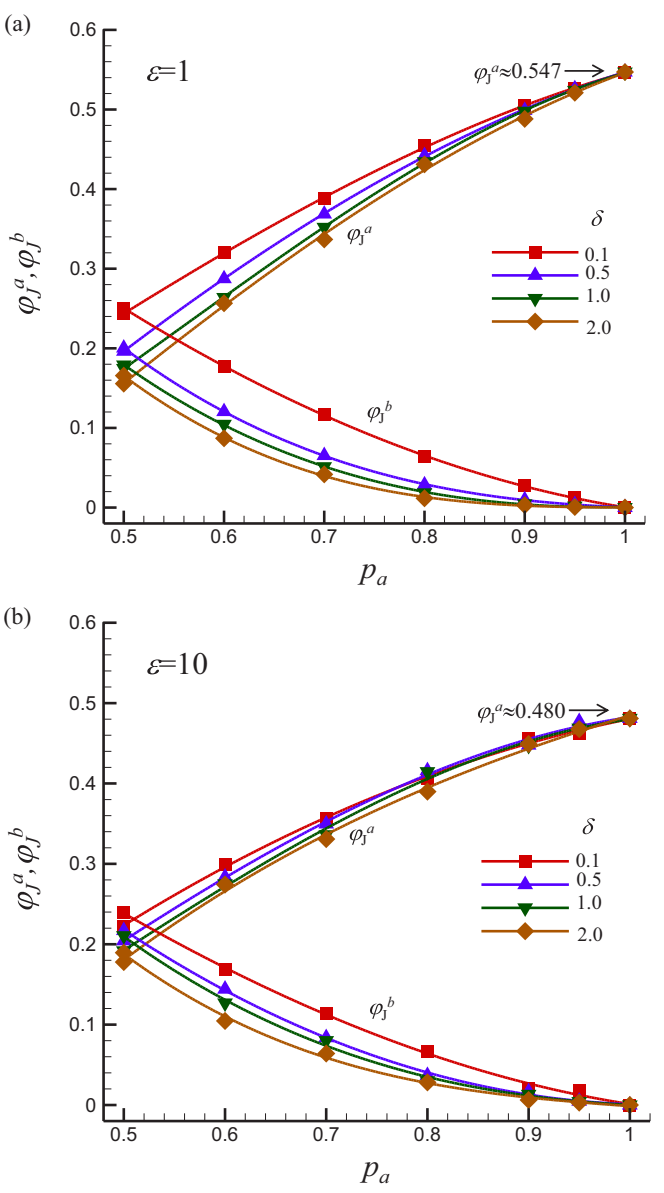


FIG. 4. Dependence of the jamming coverage φ_J^a and φ_J^b on the probability p_a for particles with aspect ratios $\varepsilon = 1$ (a) and 10 (b). Shell thickness values are $\delta = 0.1, 0.5, 1, 2$. System size $L = 128$.

Figure 5 shows the total jamming coverage φ_J as a function of the aspect ratio ε for different shell thicknesses δ and two probability values, $p_a = 0.5$ (a) and 0.7 (b). For comparison, the dependence $\varphi_J(\varepsilon)$ at $\delta = 0$, corresponding to the single-component RSA model, is also shown. In the single-component model, $\varphi_J(\varepsilon)$ exhibits a maximum at $\varepsilon \approx 1.8$. In the antagonistic model, a similar trend is observed; however, both the maximum value of the jamming coverage and the position of the maximum depend on the shell thickness δ. The dotted lines indicate the positions of the maxima for different δ. As δ increases, the maximum shifts toward larger values of ε. Moreover, this shift in the position of the maximum is more pronounced for $p_a = 0.5$ than for $p_a = 0.7$.

B. Percolation

Figure 6 shows the dependence of the percolation shell thickness δ_c on the probability p_a for shell thicknesses $\delta = 0.5$ and $\delta = 1$ and two aspect ratios $\varepsilon = 1$ and $\varepsilon = 10$. The percolation thickness δ_c decreases with increasing p_a. This behavior occurs because, as p_a increases, the model approaches the single-component RSA, and the effect of the repulsive shell δ becomes negligible. For the single-component RSA ($p_a = 1$), the percolation thicknesses for $\varepsilon = 1$ and 10 are approximately $\delta_c \approx 0.084$ and 0.163, respectively [37,38].

For each combination of ε and δ, the critical probability p_a^c is defined by the condition $\delta_c = \delta$. The horizontal dashed line in Fig. 6, which intersects the curve $\delta_c(p_a)$ at $\varepsilon = 1$ and $\delta = 1$, illustrates the method for determining p_a^c. As noted above, in this model, clusters of different particle types are separated

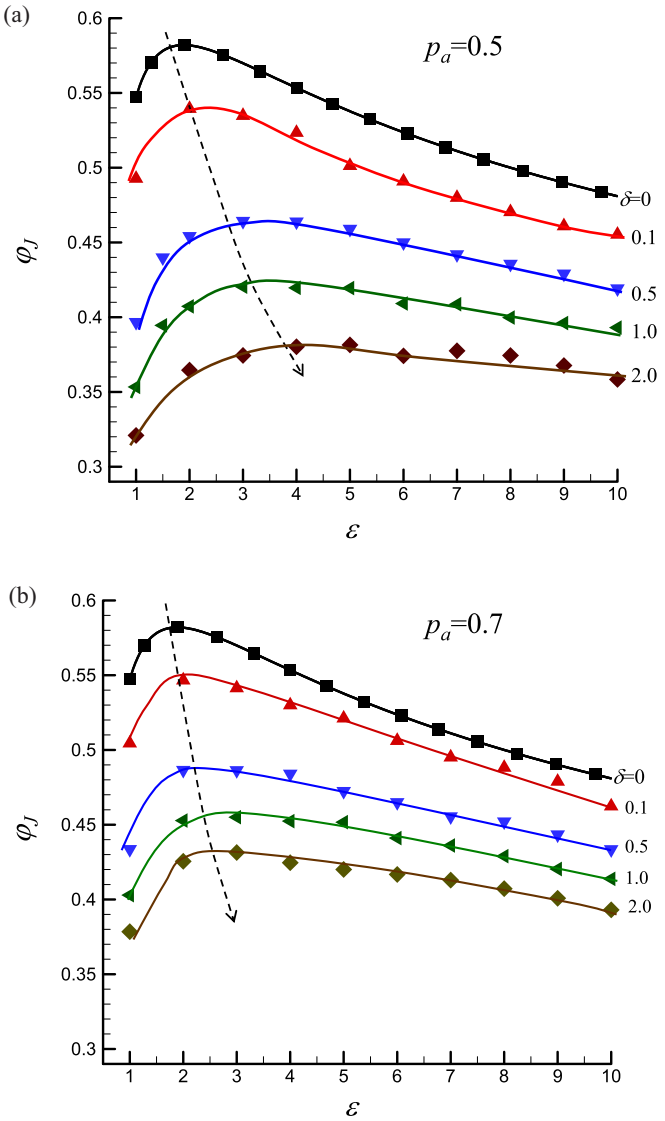


FIG. 5. Dependence of the total jamming coverage φ_J on the aspect ratio ε for different shell thicknesses δ and two probability values, $p_a = 0.5$ (a) and 0.7 (b). The dotted lines indicate the positions of the maxima for different δ. System size $L = 128$.

by cavities of average thickness $\approx 2\delta$ (see Fig. 1). Therefore, it is reasonable to assume that the percolation shell thickness within a cluster of particles of the same type, δ_c, should not exceed the repulsive shell thickness, i.e., $\delta_c \leqslant \delta$. Values of $\delta_c > \delta$ in Fig. 6 indicate that percolation occurs through the merging of separate clusters of type a particles. For example, for the curve $\delta_c(p_a)$ at $\varepsilon = 1$ and $\delta = 1$, the critical probability is $p_a^c \approx 0.54$.

In the single-component RSA model, as shown in Fig. 4, the coverage for individual particle types is higher due to the absence of channels between clusters of particles of different types. That is, the average distance between particle surfaces is smaller, and accordingly, δ_c decreases with increasing p_a. A significant influence of the repulsive shell thickness δ for different aspect ratios ε is observed only in the region $0.5 \leqslant p_a \lesssim 0.6$, where competition between adsorption of the two particle types is maximal.

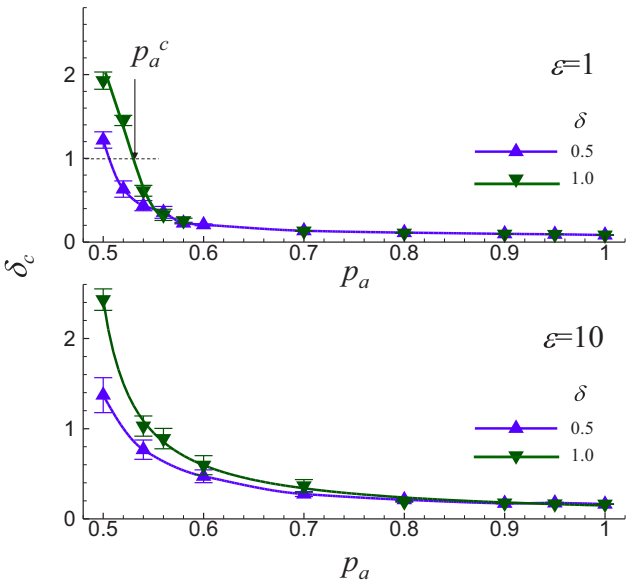


FIG. 6. Dependence of the percolation shell thickness δ_c on the probability p_a for shell thicknesses $\delta = 0.5$ and 1 and two aspect ratios $\varepsilon = 1$ and $\varepsilon = 10$. The horizontal dashed line, which intersects the curve $\delta_c(p_a)$ at $\varepsilon = 1$ and $\delta = 1$, illustrates the method for determining the critical probability p_a^c (see text for details). System size $L = 128$.

Figure 7 shows the dependence of the critical probability p_a^c on the shell thickness δ for two aspect ratios, $\varepsilon = 1$ and 10. The critical probability p_a^c decreases with increasing δ, while for a fixed δ, p_a^c increases with increasing aspect ratio ε. Sharp changes in p_a^c are observed at small shell thicknesses, $\delta \lesssim 0.5$. This behavior indicates that, at weak interparticle repulsion (small δ), the percolation behavior of the adsorption layer is highly sensitive to the presence of impurities (i.e., particles of

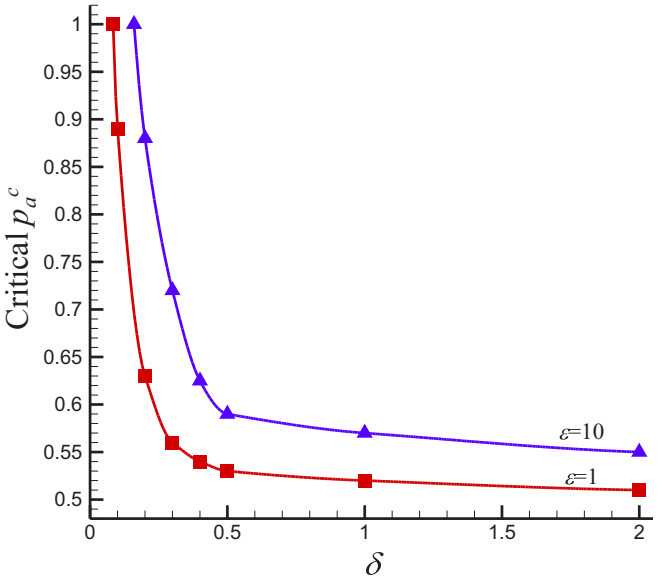


FIG. 7. Dependence of the critical probability p_a^c on the thickness of the repulsive shell δ for two aspect ratios, $\varepsilon = 1$ and $\varepsilon = 10$. System size $L = 128$.

type b). In contrast, at strong repulsion (large δ), percolation occurs only when the concentration ratio of the two particle types above the adsorbent surface is approximately equal, corresponding to the interval $0.5 \leqslant p_a^c \lesssim 0.6$.

IV. CONCLUSIONS

In this work, the antagonistic RSA model to describe the competitive adsorption of two particle types, a and b, on an adsorbent surface is analyzed. The degree of competition between particles was characterized by the probability p_a ($p_b = 1 - p_a$) that the next particle arriving at the surface would be of type a. Particles of both types were modeled as discorectangles with an aspect ratio $\varepsilon = l/d$, where l and d are the particle length and thickness, respectively. Each particle was surrounded by a shell of thickness δ, which induced repulsion between particles of opposite types (preventing overlap of shells during adsorption) but did not affect particles of the same type.

For this model the self-assembly of clusters of the same particle type on the adsorbent surface, with clusters separated by cavities of thickness approximately 2δ, is observed. The adsorption layer formation process can be divided into two stages, separated by the maximum on the derivative curves of coverage versus time. The first stage is characterized by the formation of cluster growth centers for each particle type, while the second stage is characterized by their enlargement.

The jamming behavior is completely symmetric and exhibits the highest competition between particle types at $p_a = 0.5$. For $p_a > 0.5$, type a particles dominate the adsorption layer, whereas for $p_a < 0.5$, type b particles dominate. The limiting cases $p_a = 0$ and $p_a = 1$ correspond to the single-component RSA model, where the maximum jamming coverage is observed for all values of δ. The probability p_a can be regarded as a parameter controlling the deviation of the antagonistic RSA model from the single-component case. At $p_a = 0.5$, the minimum surface coverage of the adsorbent by both particle types is observed, and this minimum decreases with increasing δ. This effect is due to the enlargement of cavities between clusters of different particle types as δ increases. For the total jamming coverage as a function of ε in the antagonistic RSA model, a maximum is observed, similar to the single-component case. Both the position and value of this maximum depend on δ, with the most pronounced shift occurring at $p_a = 0.5$.

The percolation shell thickness δ_c was analyzed as a function of p_a for various values of δ and ε. It was found that δ_c decreases with increasing p_a, as the model approaches the single-component RSA and the effect of the repulsive shell δ diminishes. The influence of δ on δ_c is significant only in the range $0.5 \leqslant p_a \lesssim 0.6$, where competition between the two particle types is maximal. For each combination of ε and δ, a critical probability p_a^c can be defined, corresponding to the condition $\delta_c = \delta$. The critical probability p_a^c decreases with increasing δ, with sharp changes observed for small repulsive shell thicknesses ($\delta \lesssim 0.5$). This indicates that, under weak repulsion (small δ), the percolation behavior is highly sensitive to the presence of impurities, whereas under strong repulsion (large δ), percolation occurs only when the concentrations of the two particle types above the adsorbent surface are approximately equal.

ACKNOWLEDGMENTS

The authors acknowledge funding from the National Academy of Sciences of Ukraine (0123U104433 and 0125U000300, N.L. and N.V.) and from the Ministry Education and Science of Ukraine (0123U101955 and 23 BF051-01 LB).

DATA AVAILABILITY

No data was used for the research described in the article.

[1] J. W. Evans, Random and cooperative sequential adsorption, Rev. Mod. Phys. **65**, 1281 (1993).
[2] Z. Adamczyk, Modeling adsorption of colloids and proteins, Curr. Opin. Colloid Interface Sci. **17**, 173 (2012).
[3] M. Sadowska, M. Cieśla, and Z. Adamczyk, Nanoparticle deposition on heterogeneous surfaces: Random sequential adsorption modeling and experiments, Colloids Surf. A **617**, 126296 (2021).
[4] P. Kubala, P. Batys, J. Barbasz, P. Weroński, and M. Cieśla, Random sequential adsorption: An efficient tool for investigating the deposition of macromolecules and colloidal particles, Adv. Colloid Interface Sci. **306**, 102692 (2022).
[5] N. I. Lebovka and Y. Y. Tarasevich, Two-dimensional systems of elongated particles: From diluted to dense, in *Order, Disorder and Criticality*, edited by Y. Holovatch (World Scientific Publishing Co Pte Ltd, Singapore, 2020), Vol. 6, Chap. 4, pp. 153–200.
[6] R. D. Vigil and R. M. Ziff, Random sequential adsorption of unoriented rectangles onto a plane, J. Chem. Phys. **91**, 2599 (1989).
[7] R. D. Vigil and R. M. Ziff, Kinetics of random sequential adsorption of rectangles and line segments, J. Chem. Phys. **93**, 8270 (1990).
[8] K. Haiduk, P. Kubala, and M. Cieśla, Saturated packings of convex anisotropic objects under random sequential adsorption protocol, Phys. Rev. E **98**, 063309 (2018).
[9] N. I. Lebovka, N. V. Vygornitskii, and Y. Y. Tarasevich, Random sequential adsorption of partially ordered discorectangles onto a continuous plane, Phys. Rev. E **102**, 022133 (2020).
[10] J. Talbot, G. Tarjus, P. Van Tassel, and P. Viot, From car parking to protein adsorption: An overview of sequential adsorption processes, Colloids Surf. A **165**, 287 (2000).
[11] J. D. Sherwood, Random sequential adsorption of lines and ellipses, J. Phys. A: Math. Gen. **23**, 2827 (1990).
[12] P. Abritta and R. S. Hoy, Structure of saturated random-sequential-adsorption ellipse packings, Phys. Rev. E **106**, 054604 (2022).
[13] R. S. Hoy, Generating ultradense jammed ellipse packings using biased SWAP, J. Phys. Chem. B **129**, 763 (2025).

[14] E. J. Perino, D. A. Matoz-Fernandez, P. M. Pasinetti, and A. J. Ramirez-Pastor, Jamming and percolation in random sequential adsorption of straight rigid rods on a two-dimensional triangular lattice, J. Stat. Mech. (2017) 073206.

[15] L. Budinski-Petković, I. Lončarević, Z. M. Jakšić, and S. B. Vrhovac, Jamming and percolation in random sequential adsorption of extended objects on a triangular lattice with quenched impurities, J. Stat. Mech. (2016) 053101.

[16] M. Cieśla, Continuum random sequential adsorption of polymer on a flat and homogeneous surface, Phys. Rev. E **87**, 052401 (2013).

[17] A. Donev, I. Cisse, D. Sachs, E. A. Variano, F. H. Stillinger, R. Connelly, S. Torquato, and P. M. Chaikin, Improving the density of jammed disordered packings using ellipsoids, Science **303**, 990 (2004).

[18] G. Tarjus and J. Talbot, Random sequential adsorption of polydisperse mixtures: Asymptotic kinetics and structure, J. Phys. A: Math. Gen. **24**, L913 (1991).

[19] P. Meakin and R. Jullien, Random-sequential adsorption of disks of different sizes, Phys. Rev. A **46**, 2029 (1992).

[20] K. V. Wagaskar, R. Late, A. G. Banpurkar, A. V. Limaye, and P. B. Shelke, Simulation studies of random sequential adsorption (RSA) of mixture of two-component circular discs, J. Stat. Phys. **181**, 2191 (2020).

[21] N. I. Lebovka, M. R. Petryk, and N. V. Vygornitskii, Percolation connectivity in deposits obtained using competitive random sequential adsorption of binary disk mixtures, Condens. Matter Phys. **27**, 13201 (2024).

[22] N. Lebovka, M. Cieśla, L. Petrone, and N. Vygornitskii, Competitive random sequential adsorption of binary mixtures of disks and discorectangles, J. Phys. A: Math. Theor. **57**, 095001 (2024).

[23] P. Weroński, Effect of electrostatic interaction on deposition of colloid on partially covered surfaces: Part I. Model formulation, Colloids Surf. A **294**, 254 (2007).

[24] N. A. M. Araújo, A. Cadilhe, and V. Privman, Morphology of fine-particle monolayers deposited on nanopatterned substrates, Phys. Rev. E **77**, 031603 (2008).

[25] Z. Adamczyk, M. Morga, M. Nattich-Rak, and M. Sadowska, Nanoparticle and bioparticle deposition kinetics, Adv. Colloid Interface Sci. **302**, 102630 (2022).

[26] N. Lebovka, M. Petryk, M. O. Tatochenko, and N. V. Vygornitskii, Two-stage random sequential adsorption of discorectangles and disks on a two-dimensional surface, Phys. Rev. E **108**, 024109 (2023).

[27] Z. Adamczyk, B. Siwek, and P. Weroński, Adsorption of colloid particles at partially covered surfaces, J. Colloid Interface Sci. **195**, 261 (1997).

[28] Z. Adamczyk and P. Weroński, Random sequential adsorption on partially covered surfaces, J. Chem. Phys. **108**, 9851 (1998).

[29] J. W. Evans, D. Hoffman, and D. Burgess, Competing irreversible cooperative reactions on polymer chains, J. Chem. Phys. **80**, 936 (1984).

[30] C. S. do Amaral and D. C. dos Santos, One-dimensional *AB* random sequential adsorption with one deposition per site, J. Phys. A: Math. Theor. **56**, 475204 (2023).

[31] J. W. Evans and D. E. Sanders, Percolative c(2×2) adlayer structure in nonequilibrium adsorption models, Phys. Rev. B **39**, 1587 (1989).

[32] S. Kundu, H. C. Prates, and N. A. Araújo, Jamming and percolation in the random sequential adsorption of a binary mixture on the square lattice, J. Phys. A: Math. Theor. **55**, 204005 (2022).

[33] P. H. L. Martins, R. Dickman, and R. M. Ziff, Percolation in two-species antagonistic random sequential adsorption in two dimensions, Phys. Rev. E **107**, 024104 (2023).

[34] P. Viot, G. Tarjus, S. M. Ricci, and J. Talbot, Random sequential adsorption of anisotropic particles. I. Jamming limit and asymptotic behavior, J. Chem. Phys. **97**, 5212 (1992).

[35] S. M. Ricci, J. Talbot, G. Tarjus, and P. Viot, Random sequential adsorption of anisotropic particles. II. Low coverage kinetics, J. Chem. Phys. **97**, 5219 (1992).

[36] Z. Adamczyk, *Particles at Interfaces: Interactions, Deposition, Structure* (Elsevier, 2017), Vol. 20.

[37] N. I. Lebovka, M. O. Tatochenko, N. V. Vygornitskii, A. V. Eserkepov, R. K. Akhunzhanov, and Y. Y. Tarasevich, Connectedness percolation in the random sequential adsorption packings of elongated particles, Phys. Rev. E **103**, 042113 (2021).

[38] N. I. Lebovka, M. O. Tatochenko, N. V. Vygornitskii, and Y. Y. Tarasevich, Confinement effects on the random sequential adsorption packings of elongated particles in a slit, Phys. Rev. E **104**, 054104 (2021).